Environ Earth Sci
DOI 10.1007/s12665-014-3937-7

ORIGINAL ARTICLE

Comparative analysis of the soil thermal regimes of typical underlying surfaces of oasis systems in an Arid Region

Yinhuan Ao · Shihua Lyu · Bo Han · Zhaoguo Li

Received: 10 June 2014 / Accepted: 7 December 2014

Abstract Using supplementary observational data obtained from the "Oasis System Energy and Water Cycle Field Experiment" conducted in the summer of 2005 and 2008, we performed a comparative analysis of the characteristics of soil thermal regimes of an Oasis and the Gobi in terms of the surface albedo, soil temperature gradient, soil heat flux and soil thermal conductivity. The results showed that on sunny summer days, the daily average albedos of the Gobi and Oasis were 0.215, 0.159 in 2005 and 0.207, 0.150 in 2008, respectively. The soil temperature gradient and the net radiation showed an approximate linear relationship; the soil temperature gradient decreased with the increase of net radiation and it declined faster when the net radiation was negative. The soil heat flux of the 0.05 m soil layer varied in phase with the soil heat flux of the 0.20 m layer of soil. The thermal conductivity values of the 0.05 m layer of the Gobi and Oasis soil were 0.193 and 0.374 W m^{-1} K^{-1}. The soil heat flux can be well estimated using soil temperature gradient and soil thermal conductivity from observation in the Gobi.

Keywords Surface albedo · Soil temperature gradient · Soil heat flux · Soil thermal conductivity

Y. Ao · S. Lyu · B. Han · Z. Li (✉)
Key Laboratory of Land Surface Process and Climate Change in Cold and Arid Regions, Chinese Academy of Sciences, Lanzhou 730000, China
e-mail: lzgnuist@163.com

Z. Li
University of Chinese Academy of Sciences, Beijing 100049, China

Introduction

The surface energy flux can change the structure of the atmospheric boundary layer as well as its mechanism (Kristovich and Braham 1998; MacKellar et al. 2013; Mahrt and Vickers 2005; Michael and Cuenca 1994; Oncley et al. 2007), and further influence the regional and global climate (Harding and Snyder 2012; Trenberth et al. 2001; Watterson and Dix 1996; Zhu and Lettenmaier 2007). The law governing interactions between the underlying surface and atmosphere in different environments have been studied for many years by meteorologists in China and throughout the world (Bernhofer 1992; Hammerle et al. 2007; Wen et al. 2014; Wu et al. 2014; Zhang et al. 2014). Soil temperature and soil heat flux are the main parameters that determine the soil thermal regime, which also significantly influence the energy balances of different ecological systems (Guo et al. 2011; Heusinkveld et al. 2004; Li et al. 2014). As one of the major components of the land–atmosphere interaction, the surface energy balance reflects the energy bonding function of the land–atmosphere coupling process (Zhang and Cao 2003). The climate change due to solar activity, land use changes and anthropogenic activities is mainly realized through changes in the radiation balance and the energy exchange between land and atmosphere. Therefore, changes in surface heating field are of significant concern in the study of global climate change and climatic anomalies (Ogée et al. 2001; Wilson et al. 2002; Zhang and Cao 2003). Undoubtedly, the land–atmosphere interaction plays an important role in climate systems, and the soil thermal regime also plays an extremely important role in the land–atmosphere interaction. A description of changes in the heat and moisture of soil is also essential for the development of land surface models (Gayler et al. 2013; Ren et al. 2008; Shao and

Published online: 14 December 2014

Irannejad 1999; Warrach et al. 2001). According to the study by Yang et al. (2005), the vertical heterogeneity of soil has a significant influence on simulations of the vertical distribution of the soil moisture content, which can in turn affect land surface model simulations of the sensible heat flux and latent heat flux. Ji and Pu (1989) conducted a study on the characteristics of surface heating fields in the Tibetan Plateau, and Li et al. (2005) discussed the characteristics of surface heating fields and soil thermal regimes in the Wudaoliang Region of the northern Tibetan Plateau. Using ground temperature data collected over many years, Zhang et al. (2005) calculated the distribution characteristics of soil heat flux in the Tibetan Plateau. Based on these data, Gao (2005) and Gao et al. (2003) described the effect of soil heat convection on soil temperature. Furthermore, Gao et al. (2010) characterized the phase difference between soil surface heat flux and temperature and to investigate whether it influences soil surface energy balance closure. These studies gave an explanation for the non-closure of the surface energy balance observed in the field experiments, which has been widely recognized. However, these studies mainly addressed conditions in the Tibetan Plateau, and few studies have focused on the arid and semiarid regions of northwestern China.

In this study, the Jinta Oasis is located in the Heihe River Basin in northwest China. In recent years, studies of the heterogeneous underlying surface of this Oasis system have been increasingly highlighted by atmospheric boundary layer research (Han et al. 2010; Meng et al. 2009). For example, the "HEIFE" and "Field Experiment on Land–atmosphere interaction in Arid Region of Northwest China" projects have been conducted in this area. In these studies, researchers determined some of the characteristics of the land–atmosphere interaction in the arid and semiarid regions of northwest China, and they put forward several new concepts on certain land surface processes (Kang et al. 2005; Tamagawa 1996; Wang and Mitsuta 1992; Zhang et al. 2002). However, further study is needed. To assess the water-heat exchange between the extremely important Jinta Oasis and the surrounding Gobi in the arid and semiarid region of northwest China, the "Oasis System Energy and Water Cycle Field Experiment" (simply called the "Jinta Experiment") was carried out in Gansu Province in China in the summers of 2005 and 2008 (Han et al. 2010). The objective was to obtain observational data from experiments at the Gobi and Oasis sites using a consistent observation system (Table 1). Here, the soil thermal regimes of different underlying surfaces based on their surface albedo, soil temperature gradient, soil heat flux and soil thermal conductivity were analyzed and discussed.

Table 1 The site and underlying surface of the observed stations

Station	Coordinates	The underlying surface
Oasis	39°59.488′N 98°56.177′E	There were cropland covered with the mature period wheat
Gobi	39°58.353′N 98°51.518′E	There were different sizes of gravel on the Gobi

Materials and methods

Study area and data selection

In this study, the Jinta Oasis is situated in the western part of the Badain Jaran Desert and along the bank of the Heihe River. The Oasis has a total area of approximately 2,152 km^2 and lies between 98°39′ to 99°08′E and 39°56′ to 40°17′N. Jinta Oasis is surrounded by the Gobi, and its topography is flat with altitude difference of only approximately 80 m (Fig. 1). This area has a temperate continental climate with an annual precipitation of approximately 59.5 mm and an annual potential evapotranspiration of approximately 2,538 mm. The soil–water recharge of the Jinta Oasis is mainly dependent on snowmelt from Qilian Mountain and irrigation through manual wells. The Jinta Oasis also receives strong solar radiation and exhibits considerable temperature differences between day and night as well as an intense land–atmosphere water and heat exchange. The data were adopted in 2005 and 2008, respectively. The observational period spanned from

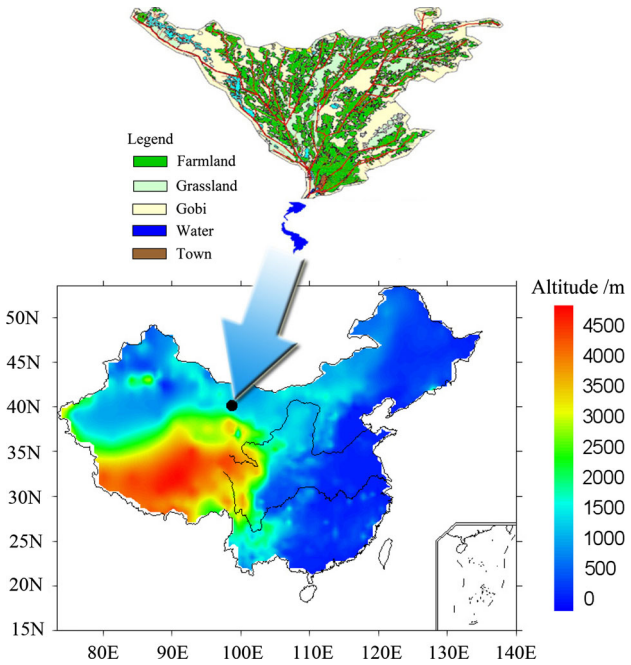

Fig. 1 Geographic and land use sketch map of Jinta Oasis

summer to autumn in 2005 and 2008. The experiments were simultaneously conducted in the Oasis and Gobi study areas. The observation variables included the downward and upward shortwave radiation, the downward and upward long-wave radiation, the latent heat flux, the sensible heat flux, the soil heat flux, the soil temperature, the soil moisture content, the air temperature and humidity. Please see Table 2 for details regarding the observation height and instruments. All instruments were calibrated, and comparative tests were conducted prior to the experiment. The results were in line across all instruments. The sampling frequency of the ultrasonic instrument was 10 Hz.

By focusing on the comparative analysis of characteristics of the soil thermal regimes of different underlying surfaces on several consecutive sunny days in June of 2005 and 2008, this paper provides a reference for studying the interaction mechanism of the soil–plant–atmosphere continuum of different underlying surfaces in the Oasis and Gobi. In this paper, the observation time was converted into the local time, with the average of the analytical data over a period of 1 h. All experimental data used in this paper passed quality control assessments.

Albedo

In this study, the average surface albedo refers to the specific value of upward shortwave radiation and downward shortwave radiation during the observation period:

$$\alpha = {}^{R}/_{Q} \tag{1}$$

In this equation, R is the upward shortwave radiation reflected from the surface, and Q is the downward shortwave radiation. Generally, the surface albedo is a function of several factors such as the surface soil color, roughness length, soil moisture content and solar elevation (Li et al. 2005). However, because diurnal variations of the surface soil color and roughness length are not evident during short-term observation, soil moisture content and solar elevation are regarded as the major factors causing the diurnal variation of the albedo.

Soil temperature gradient and surface net radiation

The soil temperature gradient reflects the variation in temperature within a unit of vertical distance. This is an important physical quantity that is indicative of the intensity of heat transmission in the vertical direction. The heat transmission takes place in the opposite direction as the soil temperature gradient.

The equation for the soil temperature gradient is as follows:

$$Gra = \frac{\partial T}{\partial Z} \approx \left\{ \frac{\Delta T_1/\Delta Z_1 + \Delta T_2/\Delta Z_2}{2} \right\} \tag{2}$$

In this equation, Gra is the soil temperature gradient in K m^{-1}, ΔT is the temperature difference (°C) between two soil layers and ΔZ is the depth interval between two soil layers. The temperature difference of the two soil layers can be calculated using Eqs. (3a, 3b):

$$\Delta T_1 = T_1 - T_0 \tag{3a}$$

$$\Delta T_2 = T_2 - T_1 \tag{3b}$$

In these equations, T_0 is the soil surface temperature, T_1 is the temperature at 0.1 m depth of soil and T_2 is the temperature at 0.2 m depth of soil. ΔZ_1 is the depth interval between 0 and 0.1 m layer of soil, ΔZ_2 is the depth interval between 0.1 and 0.2 m layer of soil, can be expressed as:

$$\Delta Z_1 = \Delta Z_2 = 0.1 \text{ m}$$

Soil heat flux and soil thermal conductivity

In this experiment, the average values measured for soil heat flux plate at 0.05 and 0.20 m depth of soil were used to express the soil heat flux at different depths in the observation sites. As an example, the diurnal variations of the soil heat flux were analyzed at different depths on a typical sunny day (June 25, 2005).

The equation for the soil heat flux is as follow:

$$G = -\lambda \frac{\partial T}{\partial Z} \tag{4}$$

In this equation, G is the soil heat flux (W m^{-2}), λ is the soil thermal conductivity (W m^{-1} K^{-1}) and $\frac{\partial T}{\partial Z}$ is the soil

Table 2 Sensors and install height of different observation instruments

Content	Instrument	Manufacturer	Country	Installation height (m)
Air temperature and humidity	HMP45C	Vaisala	Finland	3.0
Radiation components	CNR-1	Kipp & Zone	Netherlands	1.5
Turbulent flux	CSAT3/LI-7500	Campbell scientific/LI-COR	USA	3.2
Soil heat flux	HFP01	Hukseflux	USA	−0.05, −0.20
Soil temperature	107L	Campbell scientific	USA	−0.05, −0.10, −0.20, −0.40
Soil moisture content	CS616	Campbell scientific	USA	−0.05, −0.10, −0.20, −0.40

temperature gradient (K m^{-1}). λ can be calculated by rearranging Eq. (5):

$$\lambda = -G/(\partial T/\partial Z) \quad (5)$$

By substituting the soil heat fluxes observed at 0.05 m depth of soil in the Gobi and Oasis (G), as well as the temperature gradient $(\partial T/\partial Z)$ calculated using the Eq. (5), the soil thermal conductivity of the 0.05 m layer could be easily obtained for different underlying surfaces.

Results and discussion

Albedo

The albedos of different underlying surfaces in the Jinta Oasis during consecutive sunny days are shown in Fig. 2a, b, and the average diurnal variation on several days as well as the fitted curve is presented in Fig. 2c, d.

The albedo is relatively high in the morning and late in the afternoon and relatively low at noon but is not symmetric around 12:00 at noon. In other words, during a single day, the albedo can vary when the solar altitude is constant, and the albedo law in the Oasis is more conspicuous than that in the Gobi. The diurnal variation curves of the albedo for the Gobi get closer to U-shaped because the soil in this area is dry and the soil moisture content is low. In addition, the diurnal variation of the albedo is a function of variations in the solar elevation.

Statistics showed that the daily average albedos of Gobi and Oasis at noon (11:00–13:00) were 0.215, 0.159 in 2005 and 0.207, 0.150 in 2008, respectively. The albedo of the Gobi was clearly higher than that of the Oasis, mainly because the shade provided by plants in the Oasis reduced the albedo; in addition, the soil of the Oasis contains more moisture, and the moisture surrounding the soil particles increases the absorption of downward shortwave radiation. Generally, higher soil moisture content corresponds with a lower albedo. The observations showed that the albedo of the Gobi region surrounding the Jinta Oasis was approximately equal to the albedo of the Heihe Region (0.228) (Zou et al. 1992).

Soil temperature gradient and surface net radiation

The soil temperature gradients of the Gobi and Oasis in the Jinta region were calculated using Eqs. (2) and (3a, 3b). Figure 3 shows the soil temperature gradients of different underlying surfaces in the Jinta region during consecutive sunny days as well as the average diurnal variation of the soil temperature gradients. Based on Fig. 3, it could identify the apparent characteristics of the diurnal variation in the soil temperature gradient for different underlying surfaces. From 0:00 to 7:00 in the morning, the Gobi and Oasis both have a positive temperature gradient, indicating that during this period, the soil heat is transmitted to the land surface from the deep soil layers. As the solar elevation gradually increases, the soil temperature gradient

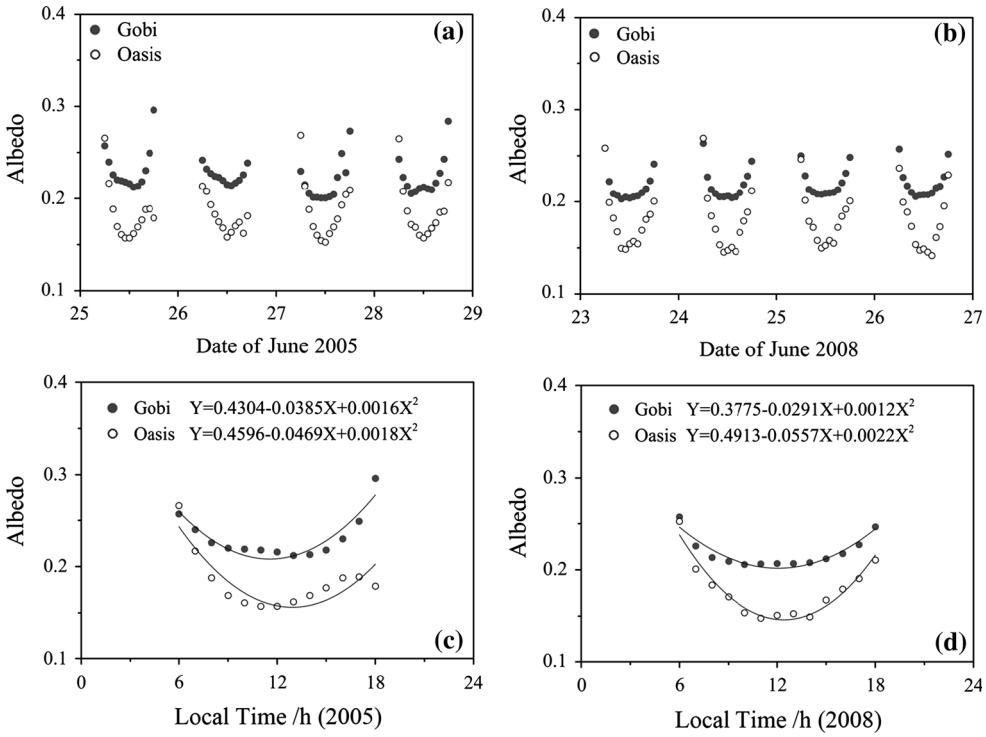

Fig. 2 Surface albedo of the different ground surface in date of June 2005 (**a**) and June 2008 (**b**), and the averaged diurnal variations (from 4 days) of surface albedo and its fitted curves in the Oasis, Gobi in 2005 (**c**) and 2008 (**d**), respectively

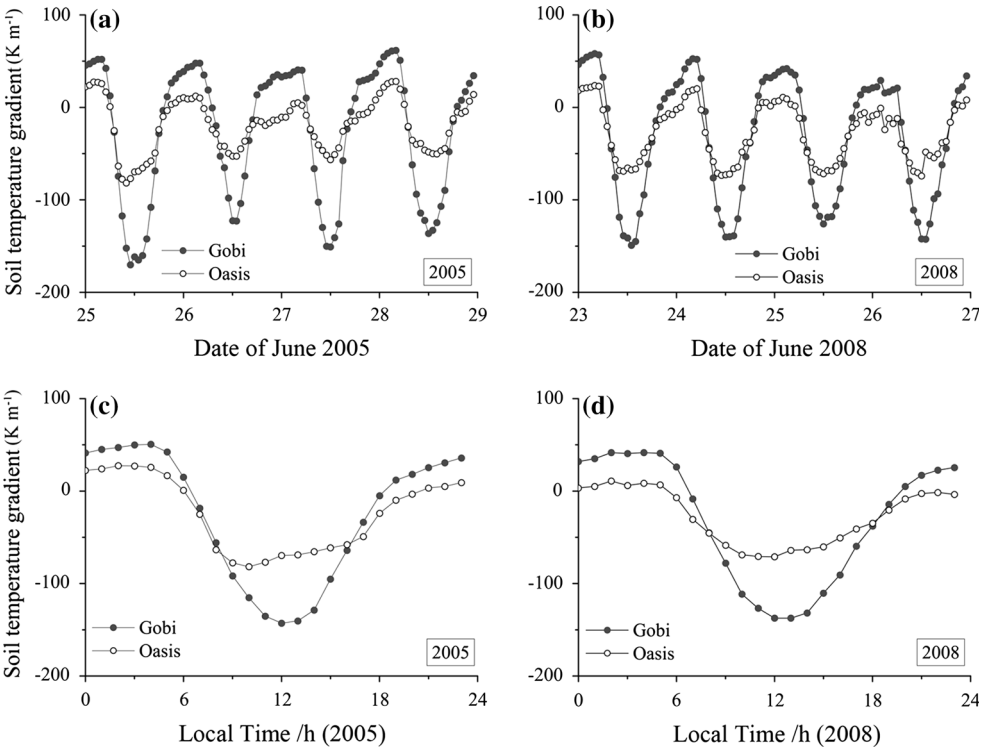

Fig. 3 Soil temperature gradient of the different ground in late June of 2005 (**a**) and 2008 (**b**), and the averaged diurnal variations (from 4 days) of the soil temperature gradient under the surface in the Oasis, Gobi in 2005 (**c**) and 2008 (**d**), respectively

turns negative, and the deeper soil receives energy from the land surface. At 19:00 in the afternoon, the soil temperature gradient again becomes positive. According to Fig. 3, the amplitude of the variation in the temperature gradient of the Oasis was clearly lower than that of the Gobi. This is mainly because the Oasis is largely covered by plants, and the plant coverage effectively reduces the solar radiation received by the land surface. Thus, the response of the soil to solar heating is delayed. At night, the long-wave radiation from the land surface of the Oasis was lower than that of the Gobi, and the land surface cooling was also relatively slow. Therefore, the variation in the soil temperature gradient of the Oasis is less obvious than that of the Gobi at night.

The diurnal variation of the soil temperature gradient mainly depends on the net radiation accepted by the land surface and the soil thermal regime (e.g., the soil moisture content, soil specific heat and soil thermal conductivity). According to the correlation analysis, the soil temperature gradient and the surface net radiation showed an approximate linear relationship (Fig. 4). Overall, the soil temperature gradient decreased with the increase in net radiation at both sites, however, it declined faster when the net radiation was negative from a microscopic view. Moreover, compared with the Oasis, there were lower soil temperature gradient (but its absolute value was large) and higher lapse rate for soil temperature gradient along with the increase of net radiation at Gobi site. The average correlation coefficients of the soil temperature gradient and net radiation for the Gobi and Oasis were −0.91 and −0.90 in both years. After fitting, we obtained the following regression equations between the soil temperature gradient (Gra) and the net radiation (R_n):

2005: Gobi

$$\mathrm{Gra} = -2.60 \times R_n + 32.32 \quad (6a)$$

Oasis

$$\mathrm{Gra} = -8.94 \times R_n + 23.66 \quad (6b)$$

2008: Gobi

$$\mathrm{Gra} = -3.25 \times R_n + 20.97 \quad (7a)$$

Oasis

$$\mathrm{Gra} = -9.01 \times R_n + 38.17 \quad (7b)$$

Soil heat flux

The diurnal variations of soil heat flux in the Gobi and Oasis as well as the variations with time and soil depth are shown in Fig. 5. The heat fluxes of the soil in the 0.05 and 0.20 m layers of the underlying surface showed diurnal variation, the variation of soil heat flux in the deep soil (0.20 m) was clearly behind that in the shallow soil (0.05 m), and its amplitude in the deep soil was small because the response of the deep soil to external influences was slow. At the Gobi site, the peak of soil heat flux at 0.05 m depth occurred at 13:00, whereas the peak of soil heat

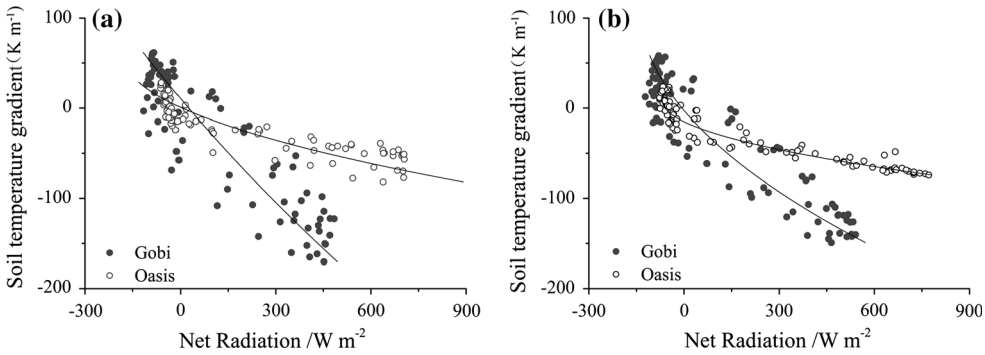

Fig. 4 The relationship between soil temperature gradient and net radiation in 2005 (**a**) and 2008 (**b**), the curves are result of quadratic polynomial fitting

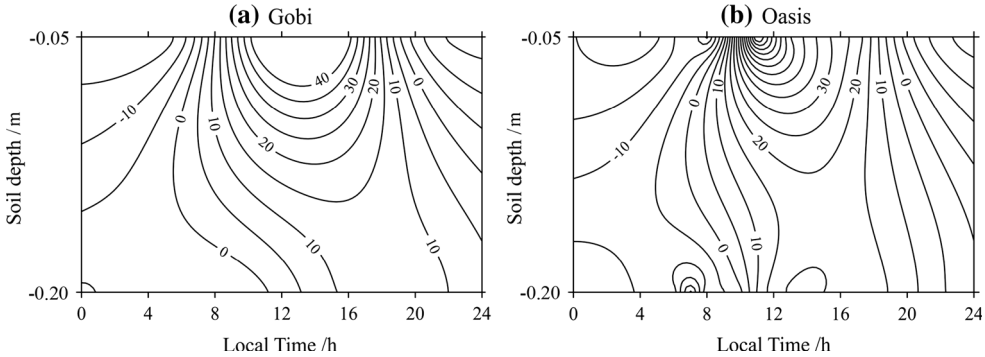

Fig. 5 Diurnal variation of soil heat flux in the Oasis and Gobi in 2005. The *solid black lines* with *number* represent the soil heat flux, unit of soil heat flux: W m^{-2}

flux at 0.20 m depth occurred at 18:00. The negative soil heat flux turned positive at approximately the same at both sites, i.e., 7:00 local time for the 0.05 m layer and 11:00 local time for the 0.20 m layer (Fig. 5a).

The 0.05 and 0.20 m layer of soil in the Oasis both showed relatively early peaks in the soil heat flux at 11:00 and 15:00, compared to the peaks at the Gobi site. The positive value of the soil heat flux in the 0.05 m layer turned negative at about 9:00 and thus lagged behind that of the Gobi. In addition to the negative soil heat flux of the 0.20 m layer turned positive at about 10:00. This demonstrates that the surface Oasis soil that is covered by plants is relatively slow to respond to external influences; however, the heat capacity is much greater owing to the high moisture content of the Oasis soil. Therefore, as the moisture gradually increases, the soil heat capacity will also increase. This fact can be regarded as a better explanation of why the soil heat flux of the 0.20 m layer in the Oasis can reach its peak value within a relatively short period. In this experiment, we only measured the soil heat flux of the 0.05 and 0.20 m layer, from which we determined the characteristics of the diurnal variation. In practice, as the soil depth increases, the characteristics of the diurnal variation in the soil heat flux become more complicated than at the land surface. For example, Zhang et al. (2005) used the ground temperature data to calculate the soil heat flux for the 0.04, 0.80 and 2.00 m layers at three stations (Amdo, Tuotuohe and Naqu) and demonstrated that the soil heat flux becomes very complicated due to variations with time and the soil depth.

Soil thermal conductivity

According to the Eq. (5), the soil thermal conductivity of the 0.05 m layer could be easily obtained for different underlying surfaces. They were 0.193 W m^{-1} K^{-1} in the Gobi and 0.374 W m^{-1} K^{-1} in the Oasis. The daily mean values of soil moisture content were 0.04 and 0.24 m^3 m^{-3}, respectively. According to these results, the soil thermal conductivity of the 0.05 m layer in the Gobi soil of the Jinta region is slightly higher than that of the Gobi soil in the Dunhuang region (Zhang et al. 2002, 2003), which is 0.177. The reason for this may lie in the fact that, when we conducted this experiment, the Oasis farmlands were in the irrigation period, and the soil moisture content was relatively high.

Based on the soil temperature gradient and soil thermal conductivity from observation, the soil heat fluxes of the 0.05 m layer were estimated by the Eq. (4) and compared to the direct measurement of soil heat flux measured by soil heat flux plate (Fig. 6). Statistics showed the correlation coefficients (r) between estimated value and observation value were 0.93 and 0.69 in the Gobi and Oasis, with the root-mean-square errors of 11.34 and 22.08 W m^{-2}, which may be related to more significant diurnal variation in the soil moisture content in the Oasis.

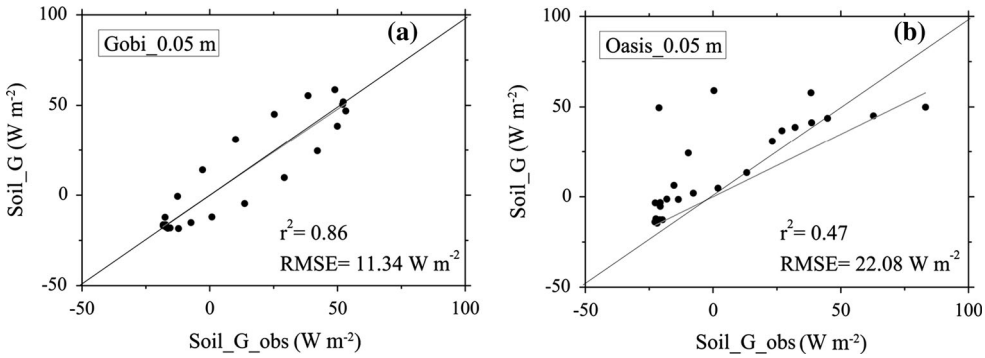

Fig. 6 The soil heat flux at 0.05 m depth in the Oasis and Gobi on 25th June in 2005: estimated by the Eq. (4) (*y axis*) versus observation (*x axis*)

Conclusions and remarks

Based on supplementary observational data obtained from the "Oasis System Energy and Water Cycle Field Experiment" conducted in the summer of 2005 and 2008, we compared the soil thermal regimes in the Jinta Oasis and the surrounding Gobi areas during several consecutive sunny days. The following conclusions are drawn:

1. The results showed a clear diurnal variation in the albedo, although the variation was not symmetric at noon (12:00). During the consecutive sunny days in summer, the daily average albedos of the Gobi and Oasis sites were 0.215, 0.159 in 2005 and 0.207, 0.150 in 2008, respectively. This difference may have occurred because the Oasis was irrigated and covered with plant during the study period. The albedo of the Gobi was approximately same as that of the Heihe region (0.228).
2. A clear diurnal variation in the soil temperature gradient of the shallow soil layers was observed. The amplitude of variation in the soil temperature gradient of the Gobi was higher than that of the Oasis. The correlation coefficients for the soil temperature gradient and surface net radiation of the Gobi and Oasis were −0.91 and −0.92, respectively.
3. Regarding the time scale of diurnal variation, the soil heat flux of the 0.05 m layer varies in phase with the soil heat flux of the 0.20 m layer. The peak value of the heat flux for the deep soil showed a clear lag behind that of the shallow soil, and this lag was more obvious in the Gobi than in the Oasis. The time of the soil heat flux of 0.05 m layer turning negative in the Oasis lagged behind that of the Gobi in the morning. This demonstrates that the Oasis soil is relatively slow to respond to external influences; because it is covered with plants and the soil heat capacity is greater owing to the high moisture content.
4. During the consecutive sunny days, the calculated thermal conductivity values of the 0.05 m layer of the Gobi and Oasis soils in the Jinta region were 0.193 and 0.374 W $m^{-1}K^{-1}$, respectively. The soil heat flux can be well estimated using soil temperature gradient and soil thermal conductivity from observation in the Gobi.

Acknowledgments This research was supported by the National Natural Science Foundation of China (grant 40975007, 41205005).

References

Bernhofer C (1992) Applying a simple three-dimensional eddy correlation system for latent and sensible heat flux to contrasting forest canopies. Theor Appl Clim 46:163–172

Gao Z (2005) Determination of soil heat flux in a Tibetan short-grass prairie. Bound Layer Meteorol 114:165–178

Gao Z, Fan X, Bian L (2003) An analytical solution to one-dimensional thermal conduction-convection in soil. Soil Sci Soc Am J 168:99–107

Gao Z, Horton R, Liu HP (2010) Impact of wave phase difference between soil surface heat flux and soil surface temperature on soil surface energy balance closure. J Geophys Res. doi:10.1029/2009JD013278

Gayler S, Ingwersen J, Priesack E, Wöhling T, Wulfmeyer V, Streck T (2013) Assessing the relevance of subsurface processes for the simulation of evapotranspiration and soil moisture dynamics with CLM3.5: comparison with field data and crop model simulations. Environ Earth Sci 69:415–427

Guo D, Yang M, Wang H (2011) Sensible and latent heat flux response to diurnal variation in soil surface temperature and moisture under different freeze/thaw soil conditions in the seasonal frozen soil region of the central Tibetan Plateau. Environ Earth Sci 63:97–107

Hammerle A, Haslwanter A, Schmitt M, Bahn M, Tappeiner U, Cernusca A, Wohlfahrt G (2007) Eddy covariance measurements of carbon dioxide, latent and sensible energy fluxes above a meadow on a mountain slope. Bound Layer Meteorol 122:397–416

Han B, Lü S, Ao Y (2010) Analysis on the interaction between turbulence and secondary circulation of the surface layer at Jinta oasis in summer. Adv Atmos Sci 27:605–620

Harding KJ, Snyder PK (2012) Modeling the atmospheric response to irrigation in the great plains. Part I: general impacts on precipitation and the energy budget. J Hydrometeorol 13:1667–1686

Heusinkveld BG, Jacobs AFG, Holtslag AAM, Berkowicz SM (2004) Surface energy balance closure in an arid region: role of soil heat flux. Agric For Meteorol 122:21–37

Ji GL, Pu M (1989) Characteristics of the surface and atmospheric heating fields over Qinghai-Xizang Plateau for the period from August 1982 to July 1983. J Meteor Res 3:228–241

Kang E, Cheng G, Song K, Jin B, Liu X, Wang J (2005) Simulation of energy and water balance in soil-vegetation-atmosphere transfer system in the mountain area of Heihe River Basin at Hexi Corridor of Northwest China. Sci China Ser D Earth Sci 48:538–548

Kristovich DA, Braham RR Jr (1998) Mean profiles of moisture fluxes in snow-filled boundary layers. Bound Layer Meteorol 87:195–215

Li R, Ji GL, Li SX (2005) Soil heat condition discussion of Wudaoliang region. Acita Energiae Solaris Sinica 26:299–304 (in Chinese with English abstract)

Li R, Zhao L, Wu T, Ding Y, Xiao Y, Jiao Y, Qin YH, Xin YF, Du E, Liu G (2014) Investigating soil thermodynamic parameters of the active layer on the northern Qinghai-Tibetan Plateau. Environ Earth Sci 71:709–722

MacKellar MC, McGowan HA, Phinn SR, Soderholm JS (2013) Observations of surface energy fluxes and boundary-layer structure over Heron Reef, Great Barrier Reef, Australia. Bound Layer Meteorol 146:319–340

Mahrt L, Vickers D (2005) Boundary-layer adjustment over small-scale changes of surface heat flux. Bound Layer Meteorol 116:313–330

Meng X, Lü S, Zhang T, Guo J, Gao Y, Bao Y, Wen L, Luo S, Liu Y (2009) Numerical simulations of the atmospheric and land conditions over the Jinta oasis in northwestern China with satellite-derived land surface parameters. J Geophys Res. doi:10.1029/2008JD010360

Michael EK, Cuenca RH (1994) Variation in soil parameters: implications for modeling surface fluxes and atmospheric boundary-layer development. Bound Layer Meteorol 70:369–383

Ogée J, Lamaud E, Brunet Y, Berbigier P, Bonnefond JM (2001) A long-term study of soil heat flux under a forest canopy. Agric For Meteorol 106:173–186

Oncley SP, Foken T, Vogt R, Kohsiek W, DeBruin HAR, Bernhofer C, Christen A, Van GE, Grantz D (2007) The energy balance experiment EBEX-2000. Part I: overview and energy balance. Bound Layer Meteorol 123:1–28

Ren D, Leslie LM, Karoly DJ (2008) Sensitivity of an ecological model to soil moisture simulations from two different hydrological models. Meteorol Atmos Phys 100:87–99

Shao Y, Irannejad P (1999) On the choice of soil hydraulic models in land–surface schemes. Bound Layer Meteorol 90:83–115

Tamagawa I (1996) Turbulent characteristics and bulk transfer coefficients over the desert in the HEIFE area. Bound Layer Meteorol 77:1–20

Trenberth KE, Caron JM, Stepaniak DP (2001) The atmospheric energy budget and implications for surface fluxes and ocean heat transports. Clim Dyn 17:259–276

Wang J, Mitsuta Y (1992) Evaporation from the desert: some preliminary results of HEIFE. Bound Layer Meteorol 59:413–418

Warrach K, Mengelkamp HT, Raschke E (2001) Treatment of frozen soil and snow cover in the land surface model SEWAB. Theor Appl Clim 69:23–37

Watterson IG, Dix MR (1996) Influences on surface energy fluxes in simulated present and doubled CO_2 climates. Clim Dyn 12:359–370

Wen Z, Niu F, Yu Q, Wang D, Feng W, Zheng J (2014) The role of rainfall in the thermal-moisture dynamics of the active layer at Beiluhe of Qinghai-Tibetan Plateau. Environ Earth Sci 71:1195–1204

Wilson K, Goldstein A, Falge E, Aubinet M, Baldocchi D, Berbigier P, Bernhofer C, Ceulemans R, Dolman H (2002) Energy balance closure at FLUXNET sites. Agric For Meteorol 113:223–243

Wu Q, Niu F, Ma W, Liu Y (2014) The effect of permafrost changes on embankment stability along the Qinghai-Xizang railway. Environ Earth Sci 71:3321–3328

Yang K, Koike T, Ye B, Bastidas L (2005) Inverse analysis of the role of soil vertical heterogeneity in controlling surface soil state and energy partition. J Geophys Res. doi:10.1029/2004jd005500

Zhang Q, Cao X (2003) The influence of synoptic conditions on the averaged surface heat and radiation budget energy over desert or Gobi. Chin J Atmos Sci 27:245–254 (in Chinese with English abstract)

Zhang Q, Cao XY, Wei GA, Huang RH (2002) Observation and study of land surface parameters over Gobi in typical arid region. Adv Atmos Sci 19:121–135

Zhang Q, Wang S, Wei G (2003) A study on parameterization of local land–surface physical processes on the Gobi of Northwest China. Chin J Geophys 46:616–623 (in Chinese with English abstract)

Zhang LJ, Li L, Shen YP (2005) A study on the soil heat flux along the Qinghai-Tibet railway based on the multi-timescale analysis. Acta Phys Sin 54:1958–1964 (in Chinese with English abstract)

Zhang YF, Wang XP, Hu R, Pan YX, Zhang H (2014) Variation of albedo to soil moisture for sand dunes and biological soil crusts in arid desert ecosystems. Environ Earth Sci 71:1281–1288

Zhu C, Lettenmaier DP (2007) Long-term climate and derived surface hydrology and energy flux data for Mexico: 1925–2004. J Clim 20:1936–1946

Zou JL, Hou XH, Ji GL (1992) Preliminary study of solar radiation properties in HEIFE area in late summer. Plateau Meteorol 114:381–388 (in Chinese with English abstract)